Damghan University Press

Journal of Nano Simulation
journal homepage: jons.du.ac.ir

Volume 2, Issue 1, Winter 2026, 56-66
DOI: 10.22128/jons.2025.3050.1014

Comparative study of intramolecular hydrogen bond strength and computational study in 3-methyl-4-amino-3-penten-2-one and 4-methylamino-3-penten-2-one

Seyedabdollah Seyedkatouli[1], Ayoub Kanaani[1*], Sahar Koukalani [2]

[1] *Department of Chemistry, Ferdowsi University of Mashhad, Mashhad, Iran*
[2]*Department of Computer Sciences, Faculty of Mathematical Sciences, University of Mazandaran, Babolsar, Iran*

HIGHLIGHTS

- IHB strengths 3-MeAPO and 4APO-NMe were investigated (theoretical and experimental).
- IHB in 3-MeAPO is stronger than in APO-NMe.
- It was found that substitution in β-ketoenamine derivatives greatly affects the IHB strengths.

GRAPHICAL ABSTRACT

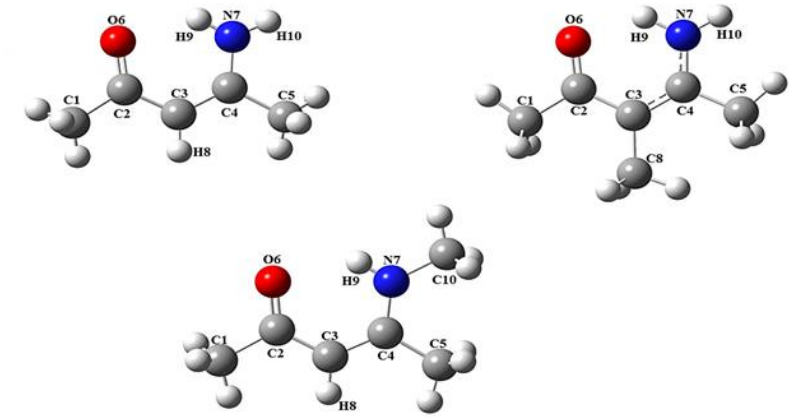

ARTICLE INFO

Article history:
Received: 2025-09-07
Received in revised form: 2025-10-05
Accepted 2026-01-26

Available online 2026-02-11

Keywords:
Methyl-4-amino-3-penten-2-one,
4-Methylamino-3-penten-2-one,
Intramolecular hydrogen bond.

ABSTRACT

The intramolecular hydrogen bond (IHB) strengths of 4-amino-3 penten-2-one (APO), 3-methyl-4-amino-3-penten-2-one (3-MeAPO) and 4-methylamino-3-penten-2-one (APO-NMe) were investigated using combined theoretical and experimental approaches. All geometry optimizations and frequency calculations were performed using density functional theory (DFT) at the B3LYP/6-31++G(d,p) level of theory, as implemented in the Gaussian 09 program package. Geometrical parameters (R, θ), spectroscopic data (IR, UV–Vis, NMR), natural bond orbital (NBO) analysis, and atoms-in-molecules (AIM) calculations were employed to evaluate and compare the IHB strength in both compounds. The most results, such as ^{1}HNMR, NH stretching, and the $E^{(2)}$, associated with the lp(O6) → σ*N7–H9 interaction confirming that the strength in APO-NMe is greater than in 3-MeAPO. In contrast, the other results, especially the X-ray data and AIM results, show different trends. These comparisons provide a clearer understanding of the effects of CH_3 substitution at the α-position and on the nitrogen atom on the strength of the intramolecular hydrogen bond (IHB). In addition, molecular electrostatic potential (MEP), frontier molecular orbital analysis (HOMO–LUMO), natural atomic charges, global reactivity parameters, and non-linear optical properties of the compound were studied using same theoretical calculations.

*a.kanaani@yahoo.com (A. Kanaani)

1- Introduction

β-Ketoenamines are a class of organic compounds of considerable interest due to their involvement in the synthesis of diverse heterocyclic and bioactive molecules. These compounds frequently exist in the aminoketone tautomeric form, where intramolecular hydrogen bonding plays a key role in stabilizing their structure and influencing their chemical reactivity. Hydrogen bonding, a critical intra and intermolecular interaction, has been extensively investigated through both theoretical and experimental approaches [1-5].

α,β Unsaturated-β-ketoenamines have in many cases been shown to exist at the aminoketone form [4, 6-8], whereas o-hydroxy Schiff bases can be tautomeric [9, 10]. The compounds can in principle exist as three different tautomers in equilibrium, i.e., iminoketone, aminoketone, and iminoenols. The aminoketone forms are usually more stable than the iminoenol forms, which are the major form of β-enaminones [4, 7, 11, 12]. The formation of an IHB leads to an increase of the resonance conjugation of the π-electrons in the chelated ring. Any factor which affects this resonance, can change the IHB strength. Synthesis, IR, and NMR spectra of some α,β-unsaturated-β ketoenamines have been already reported [2, 6, 13-15].

They are also used in the synthesis of antibiotics, anti-allergic, antiphlogistic, antitumor substances, as ligands in coordination chemistry [16]. These properties arise via H-atom transfer from the hydroxy O atom to the imine N atom [17]. It has been offered that photochromic molecules are non-planar, while thermochromic molecules are planar [18]. In general, Ketoenamines exhibit two possible tautomeric forms; O–H…N in phenol-imine (OH) [19] and N–H…O in keto-amine (NH) [20] forms are observed. In addition, non-linear properties of these molecules use in the design of various molecular electronic devices such as optical communication, optical switches, optical computing, dynamic image processing and optical data storage devices [21-23].

Several useful agents such as type of α and β substitutions, the polarity of the solvent, steric characteristics, and temperature may alter the IHB strength. Factors affecting the strength of IHB have been investigated using experimental methods (NMR, UV, Raman, IR spectroscopies, etc) and theoretical method (quantum-mechanical computing) [4, 24-29]. DFT is generally used to calculate the NBO, vibrational frequencies, electronic properties, thermodynamic functions, molecule geometry, dipole moment, reactive descriptors, atomic charges, and etc. [17, 27, 30].

Recently, the alkyl substitution effect on the α-position and nitrogen atom of APO was reported. According to these works, the methyl substitution in the α-position increased the IHB strength, while the substitution of methyl group with ethyl group on nitrogen atom had no important effect on the IHB strength [31, 32].

The aim of this study is to compare the intramolecular hydrogen bond (IHB) strength of the titled molecules. In 3-methyl-4-amino-3-penten-2-one (3-MeAPO), the methyl group is located at the α-position, whereas in 4-methylamino-3-penten-2-one (APO-NMe), the methyl group is attached to the nitrogen atom, see figure 1 for the optimized structure and their numbering. These methyl substituents may significantly influence the strength of the IHB. Therefore, a comparative investigation of their IHB strengths using both theoretical and experimental approaches may provide deeper insights into the effects of such substitutions on intramolecular hydrogen bonding.

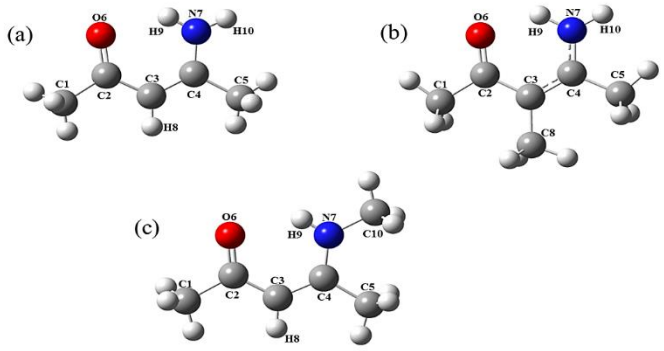

Figure 1. The optimized structure of a) APO, b) 3-MeAPO, and c) APO-NMe with their atomic numberings.

Theoretical analyses were carried out, including optimized configurations, geometric parameters, simulated vibrational and UV spectra, ^{1}H NMR chemical shifts, natural bond orbital (NBO) analysis, and atoms-in-molecules (AIM) analysis [33].

These results were then compared with experimental data obtained from IR, ^{1}HNMR, and UV–Vis spectroscopy for the titled molecules. These comparisons provide a clearer understanding of the effects of CH_3 substitution at the α-position and on the nitrogen atom on the strength of the intramolecular hydrogen bond (IHB).

Also, in the present work, the molecular structure, E_{HOMO} (the highest occupied molecular orbital energy), E_{LUMO} (the lowest unoccupied molecular orbital energy), LUMO–HOMO energy gap, global hardness (η), softness (μ), electronegativity (χ), dipole moment (μ), polarizabilities (α_{tot}), the anisotropy of the polarizabilities ($\Delta\alpha$), and the first-order hyperpolarizabilities ($<\beta>$) and molecular electrostatic potential maps (MEP) are calculated and discussed.

2. Computational studies

A portion of the theoretical and experimental data employed in this study was obtained from previously published literature [31, 32]. To complement these findings, additional quantum chemical calculations were carried out to generate the data not available in the references. All geometry optimizations and frequency calculations (in gas phase) were performed using density functional theory (DFT) at the

B3LYP/6-311++G(d,p) level of theory [34, 35], implemented in the Gaussian 09 program package [36]. For the B3LYP functional, we also applied the ‘‘D3’’ correction of Grimme et al. in conjunction with the Becke–Johnson damping function [37-39]. Also, all optimization calculations for compounds were performed by aid of OPT=Very Tight and INT=Ultrafine options.

The vibrational frequencies were calculated and scaled down by the suitable scaling factor. In the present study, a selective scaling factor of 0.9961 was used for wavenumbers >1700 cm^{-1} and 0.9556 was used for <1700 cm^{-1} at 6-311++G(d,p) [40].

The nuclear magnetic resonance (NMR) chemical shift calculations were performed using gauge-included atomic orbital (GIAO) method [41] at B3LYP/6-311++G(d,p) level in chloroform solution by the SCRF-PCM [42], and the ^1H chemical shifts were referenced to the corresponding values for TMS, which were calculated at the same levels of theory. The absorption spectra of the molecules were calculated using time-dependent density functional theory (TD-DFT) method [43] in ethanol and acetonitrile solution by the SCRF-PCM [42] method.

The changes in electron density in the σ* and π* antibonding orbitals and stabilization energies E(2) have been calculated by NBO analysis to acquire clear evidence of stabilization originating in the hyperconjugation of hydrogen-bonded interaction. Second order interaction energies (E^2) [44] and the percentage of s atomic orbital in the Lp(2)O molecular orbitals were performed at the same level, using NBO 5.0 software [45], and the natural orbitals were pictured by the Chem Craft program [46]. These help to understand substitution effects on the IHB strength. AIM 2000 software was applied to obtain the electron density (ρ) and Laplacian ($\nabla^2\rho$) of electron density at the hydrogen bondcritical points (BCP), according to Bader's AIM theory [33] at the above level of theory in addition to the IHB strength. For this purpose, first calculate the Gaussian at the B3LYP/6-311++G(d,p) level and generate the wfn files, then call the files generated by the AIM software and calculate the AIM analysis.

3.Results and discussion

Intramolecular hydrogen bonding

For a comprehensive comparison, and in accordance with previous studies [47, 48], the theoretical and experimental spectroscopic, topological, NBO, and geometrical parameters related to the IHB strength of titled molecules and APO compounds are summarized in Table 1.

In this section, the results presented in Table 1 are discussed and classified into several parts. First, the calculated and experimental

Table 1. Some selected theoretical and experimental parameters, in parentheses, of APO, APO-NMe and 3-MeAPO calculated at B3LYP/6-311++G(d,p) level of theory.

Parameters	APO		APO-NMe		3-MeAPO	
	Theoretical	Exp.	Theoretical	Exp.	Theoretical	Exp.
Spectroscopic results[a]						
δNH	10.89	9.71[b]	11.63	10.63[c]	11.39	10.32[b]
νNH	3354	3375[b]	3349	3321[d]	3693	3367[b]
UV	265	299[e]	274	---	276	319[b]
Geometricalresults[f]						
RN5-H9	1.017	0.898	1.023	0.880	1.019	0.923
RN5-H9···O1	2.937	2.890	2.855	2.907	2.837	2.797
RO1···H9	1.920	1.992	1.832	2.026	1.818	1.874
RN5···O1	2.687	2.690	2.664	2.702	2.607	2.619
θO1H9N5	129.8	133.5	135.9	132.6	131.4	135.8
AIM results[g]						
□	0.030	---	0.036	---	0.038	---
□^{2}ρ	-0.0277	---	-0.0311	---	-0.0359	---
E_{HB}	7.42	---	9.68	---	10.32	---
NBO results						
lp(2) O6→σ*(N-H)	8.19	---	11.78	---	11.26	---
Percentage of s atomic orbital	1.19	---	2.07	---	2.08	---

[a] δ, proton chemical shift in ppm; ν, is stretching bending frequence in cm^{-1}; absorption wavelength in nm.
[b] Data from Ref. [7].
[c] Data from Ref. [8].
[d] Data from Ref. [17].
[e] Data from Ref. [18].
[f] R is the intramolecular O···N, N–H, O···H distances in Å, θ:the hydrogen bond angle N–H…O in degree.
[g] Charge density (ρ) in $e.au^{-3}$, Laplacian of charge density (□^{2}ρ) in ($e.au^{-5}$) at the bond critical point (BCP) of the O/H bond. E_{HB} is the IHB energy in kcal/mol, according to Espinosa et al. suggestion [19].

spectroscopy results will be compared. With increasing IHB strength, due to greater delocalization in the chelated ring (HNCCCO), the NH chemical shift (see Figure 2) and the UV band (see Figure 3) of the chelated ring will shift to higher chemical shifts and wavenumbers, while the NH stretching vibration will appear at lower wavelengths.

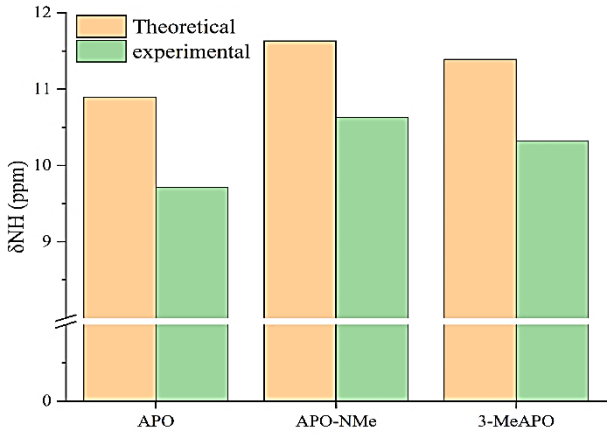

Figure 2 Compartion of tchemical shifts of APO, APO-NMe, and 3-MeAPO.

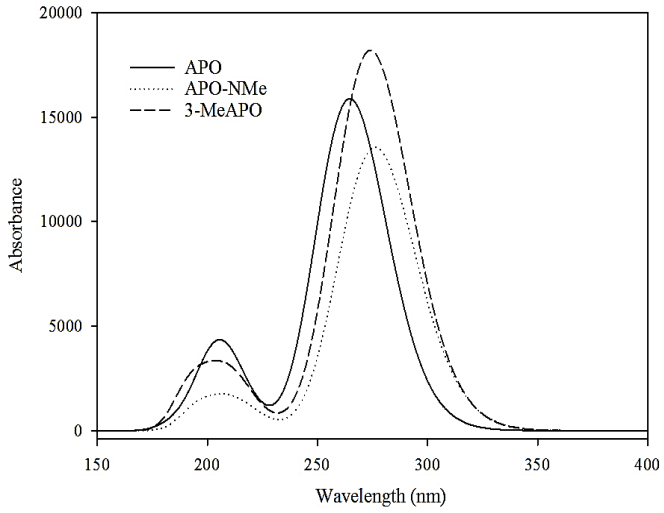

Figure 3. Comparing of APO, APO-NMe, and 3-MeAPO theoretical UV–visible absorption spectra theoretical.

According to Table 1, both calculated and experimental δNH results confirmed that IHB strength of APO-NMe is more than that 3-MeAPO. In the NH stretching of APO, since two hydrogen atoms are bonded to nitrogen, the NH stretch is not a suitable parameter to compare the IHB strength of titled molecules with APO, while both experimental and theoretical NH str. show the IHB strength of APO-NMe is upper than that 3-MeAPO.

Geometrical parameters, both experimental and theoretical, are examined as the second focus. In this section, various geometrical parameters related to IHB strength are discussed, including: N-H bond length, N-H···O, O···H, and N···O bond distance, and NHO bond angle. As the IHB strength increases, the NHO bond angle widens toward 180°, indicating a more linear and consequently stronger hydrogen bond. This strengthening is accompanied by a shortening of the O···H, N···O, and N–H···O distances, while the N–H bond length becomes slightly elongated. According to Table 1, all the theoretical structural parameters, except for the O1···H9 and N5···O1 bond distances, indicate that the IHB strength is greatest in APO-NMe. However, nearly all of the experimental X-ray results disagree with the calculated values and with the NMR chemical shifts used to confirm the IHB strength.

The calculated electron density and the corresponding Laplacian at the bond critical point (BCP) of the titled molecules were employed to characterize the intramolecular N7–H9···O6 hydrogen bonds, see Table 1.

A molecular graph of the APO is shown in Figure 4. As indicated, in addition to usual bonds, the molecular graphs indicate a BP and a BCP between nitrogen and hydrogen, which confirms that there is an intramolecular hydrogen bond (H-bond) in these molecules. Interestingly, each BCP contains a wealth of chemical information that properly describes the nature of the corresponding chemical bond.

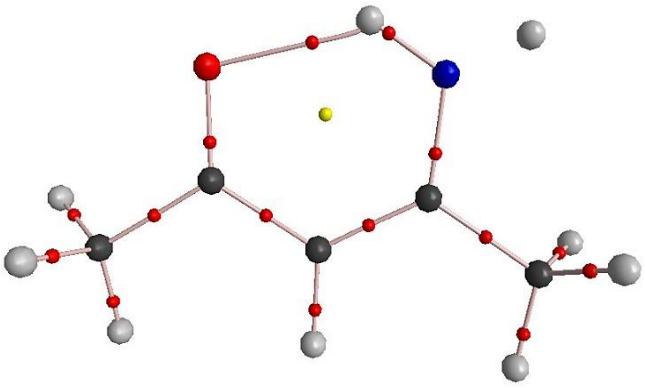

Figure 4. Molecular graphs of APo, red points indicate the bond critical points (BCPs) between bonded atoms. (For interpretation of colour,there ader is referred to the web version of this article)

In addition, the hydrogen bond energies (E_{HB}), calculated using Espinosa's equation [49] with AIM software, are reported in Table 1. Since a greater electron density and its corresponding Laplacian at the RCP indicates a stronger intramolecular hydrogen bond, and considering the calculated topological parameters presented in Table 1, it can be concluded that the hydrogen bond strength in 3-MeAPO is greater than in APO-NMe, which are not agree with the calculated and experimental spectroscopy parameters and calculated geometry parameters.

NBO analyze is provides an effective way for studying intra and inter-molecular bonding and interaction among bonds, for example, hydrogen bonding, and also provides a convenient basis for

investigating delocalisation of electron density from occupied Lewis-type (donor) NBOs to properly unoccupied non-Lewis type (acceptor) NBOs within the molecule [50]. NBO analysis has been performed on the molecule at the DFT (B3LYP)/6-311++G(d,p) level to elucidate the intra-molecular, rehybridization and delocalization of electron density within the molecule. The interactions result in a loss of occupancy from the localized NBO of the idealized Lewis structure into an empty non Lewis orbital. For each donor (i) and acceptor (j), the stabilization energy $E^{(2)}$ associated with the delocalization $i \rightarrow j$ is determined as

$$E^{(2)} = \Delta E_{ij} = q_i \frac{(F_{ij})^2}{(E_j - E_i)^2}$$

where q_i is the donor orbital occupancy, E_i and E_j are diagonal elements and F_{ij} is the off-diagonal NBO Fock matrix element. In NBO analysis, large $E^{(2)}$ value shows the intensive interaction between electron donors and electron acceptors and greater the extent of conjugation of the whole system.

The energy between an occupied Lewis type (lone pair) NBO orbital and an unoccupied (antibonding) non-Lewis NBO orbital can be a criterion to estimate an IHB strength *via* the second-order perturbation theory [51].

Natural bond orbital (NBO) analysis, particularly the second-order perturbation energies, $E^{(2)}$, associated with the intramolecular charge transfer from the lone pair on O6 (proton acceptor) to the antibonding orbital of N7–H9 (proton donor), lp(O6) → σ*N7–H9, provides valuable insight into IHB strength. The $E^{(2)}$ value for APO-NMe is greater than that for 3-MeAPO, confirming that the IHB in 3-MeAPO is stronger, that is in agreement with the other parameters. Therefore, by considering the hydrogen bond strength, the electron resonance in the chelated ring increases, the aforementioned trend for hydrogen bond strength can be concluded. The mentioned values for APO, MeAPO, and APO-NMe are 8.19, 11.266, and 11.78 kcal/mol, which follow the trend found in the calculated and experimental spectroscopy parameters and some theoretical calculated. Therefore, the trend in the hydrogen bond strength is concluded as follows: APO-NMe >APO>3-MeAPO. The hyper conjugation pictures associated with the N—H···O hydrogen bonds and the n··· σ* interaction are depicted in Figure 5.

Figure 5. The depiction of hyperconjugation interactions associated with lone pair of O atom and σ*N—H bond.

An increase in the s-character of the Lp(2)O orbital suggests enhanced σ-type overlap, which favors greater linearity of the O–H···O hydrogen bond [52]. In the LP(2)O → σ*O–H interaction shown in Table 1, the LP(2)O molecular orbitals of 3-MeAPO and APO-NMe contain 2.08 % and 2.07 % p, s character, respectively. These s-character percentages indicate that their IHB strengths are similar, which is inconsistent with the observed differences in IHB strength among the title molecules.

Molecular electrostatic potential (MEP) surface

In order to investigate the chemical reactivity of the molecule, molecular electrostatic potential (MEP) surface is plotted over the optimized electronic structure of APO, APO-NMe, and 3-MeAPO forms using density functional B3LYP level with 6-311++G(d,p) basis set. MEP is related to the electronic density and is a very useful descriptor in understanding sites for electrophilic and nucleophilic reactions as well as hydrogen bonding interactions [53-55]. The electrostatic potential V*(r)* is also well suited for analyzing processes based on the ‘‘recognition’’ of one molecule by another, because it is through their potentials that the two species first ‘‘see’’ each other [56].

The negative (red) regions of MEP were related to electrophilic reactivity and the positive (blue) regions to nucleophilic reactivity (Figure 6). Figure 6 shows the computationally observed MEP surface map with the fitting point charges to the electrostatic potential V*(r)* for title compounds. The different values of the electrostatic potential at the surface are represented by different colors. Potential increases in the order red < orange < yellow < green < blue. The predominance of the light green region in the MEP surface corresponds to a potential halfway between the two extreme regions red and dark blue color. These sites give information about the region where the compound can have intermolecular interaction. A negative electrostatic potential region is observed around the O atoms. lso a maximum positive region is localized on the hydrogen atoms indicating a possible site for nucleophilic attack. The MEP map shows that the negative potential sites are on electronegative atoms as well as the positive potential sites are around the hydrogen atoms. The MEP provides a visual representation of the chemically active sites and comparative reactivity of the atoms.

The values of the electric potential (a.u) and charges (e) of APO, APO-NMe, and 3-MeAPO are reported in Fig 6. The maximum negative sites in APO calculated at B3LYP/6311++G(d,p) is about − 22.413 (a.u) with point charge − 0.660 e.

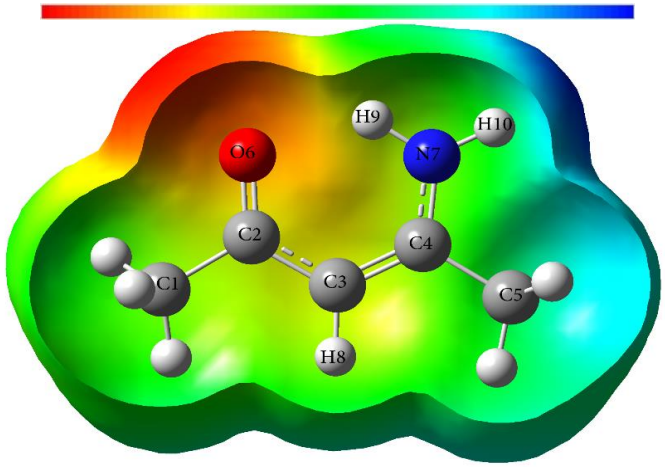

	Charges (e)	Electric Potential (a.u)
C 1	-0.649	-14.787
C 2	0.512	-14.710
C 3	-0.440	-14.796
C 4	0.287	-14.709
C 5	-0.611	-14.757
O 6	-0.658	-22.411
N 7	-0.760	-18.372
H 8	0.206	-1.114
H 9	0.438	-1.026
H 10	0.380	-1.013

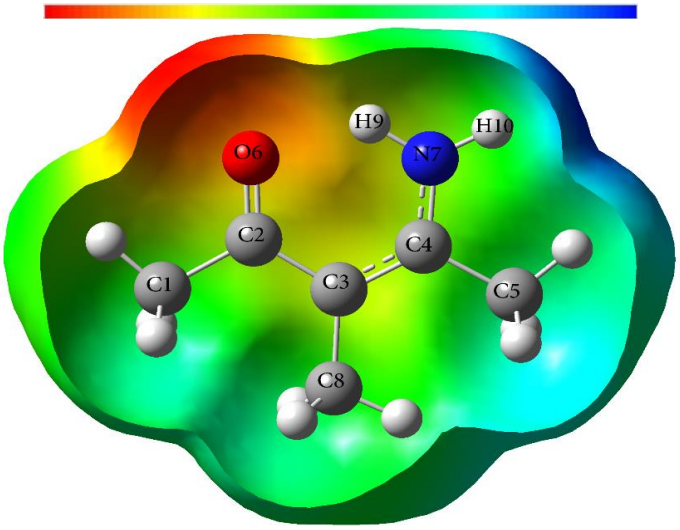

	Charges (e)	Electric Potential (a.u)
C 1	-0.652	-14.788
C 2	0.520	-14.712
C 3	-0.264	-14.787
C 4	0.285	-14.713
C 5	-0.613	-14.758
O 6	-0.660	-22.413
N 7	-0.752	-18.379
C 8	-0.581	-14.778
H 9	0.439	-1.033
H 10	0.377	-1.019

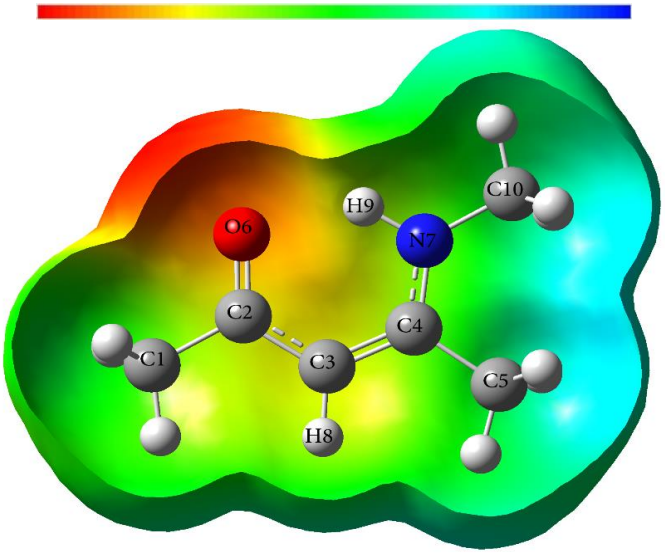

	Charges (e)	Electric Potential (a.u)
C 1	-0.646	-14.840
C 2	0.505	-14.731
C 3	-0.441	-14.824
C 4	0.306	-14.714
C 5	-0.615	-14.799
O 6	-0.673	-22.431
N 7	-0.594	-18.379
H 8	0.205	-1.131
H 9	0.440	-1.045
C 10	-0.364	-14.767

Figure 6. Molecular electrostatic potentialmap (MEP) of APO, 3-MeAPO, APO-NMe. (For interpretation of the references to colour in this figure, the reader is referred to the web version of the article.)

electrostatic potential is prominent over O6 atom. For example, the maximum negative electrostatic potential value for these electrophilic

The MEP is best suited for identifying sites for intra and inter-molecular interactions [57-59]. Also the hydrogen atoms illustrate

suitable sites for nucleophilic attack. These sites give information about the region where the compound can have intramolecular interaction. For the MEP surface of the studied molecules, the strong negative regions associated with the O6 atom and also the weak positive region by the nearby H9 atom are indicative of intramolecular (O6···H9–N7) hydrogen bonding. Based on the numbers in Figure 6 (electric Potential and charge) for the oxygen and hydrogen atoms, it can be concluded that the IHB strength is greatest in APO-NMe.

Table 2: Calculated energy values of APO, APO-NMe and 3-MeAPO calculated at B3LYP.6-311++G(d,p) level of theory.

	APO	3-MeAPO	APO-NMe
E_{HOMO} (eV)	-6/119	-5/733	-5/840
E_{HOMO-1} (eV)	-6/596	-6/517	-6/480
E_{LUMO} (eV)	-1/095	-0/892	-0/983
E_{LUMO+1} (eV)	-0/478	-0/461	-0/479
$E_{HOMO–LUMO}$ gap (eV)	5/024	4/841	4/857
chemical potential (μ)	3/607	3/312	3/412
global hardness (η)	2/512	2/420	2/428
global softness (S)	0/199	0/207	0/206
elecronegativity (χ)	-3/607	-3/312	-3/412
electrophilisity indices (ω)	2/590	2/267	2/397

Table 3: Theoretical absorption wave length λ_{max}(nm) and oscillator strengths (f) of APO, APO-NMe and 3-MeAPO using TD-DFT/6-311G++(d, p).

	Gas phase		Ethanol		Major contribution	Assignment
	λ_{max}(nm)	(f)	λ_{max}(nm)	(f)		
APO	259	0.316	265	0.392	H→L(98%)	n→π*
APO-NMe	267	0.380	274	0.448	H→L(99%)	n→π*
3-MeAPO	269	0.271	276	0.331	H→L(99%)	n→π*

Electronic properties and Global reactivity parameters

The energy gap between HOMO and LUMO is a critical parameter in characterizing molecular electrical transport properties [60]. The energy gap between the HOMO and LUMO for APO, APO-NMe, and 3-MeAPO is 5.024, 4.841, 4.857 eV, respectively (see Figure ٧). This big energy gap conforms that structure of the title compound is very stable [61].

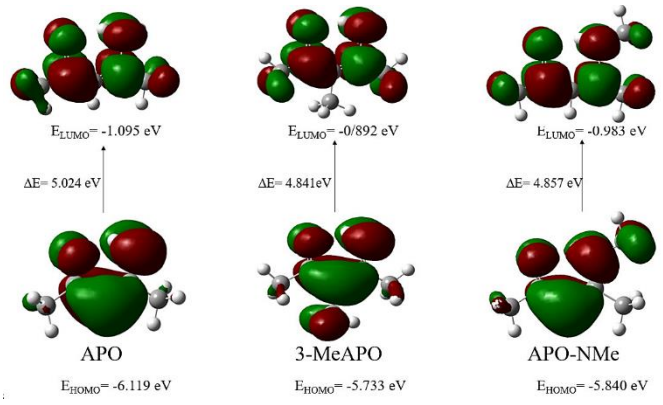

Figure 7. The atomic orbital compositions of the frontier molecular orbital for APO, APO-NMe, and 3-MeAPO.

The energy gap between the HOMO and LUMO is very important for determining the electrical properties, kinetic stability, optical polarisability and chemical reactivity descriptors, such as hardness and softness, of a molecule. On the basis of Koopman's theorem [62], global reactivity descriptors such as Electronegativity (χ)= – 1/2(E_{LUMO}+ E_{HUMO}), chemical potential (μ) = 1/2(E_{LUMO}+ E_{HUMO}), global hardness (η) = 1/2 (E_{LUMO}– E_{HUMO}), global softness (S) = 1/2η and electrophilicity index (ω)= $\mu^2/2\eta$ are calculated using the energies of frontier molecular orbitals E_{HUMO}, E_{LUMO} [63] of APO, APO-NMe, and 3-MeAPO have been listed in Table 2 and showed in Figure 8.

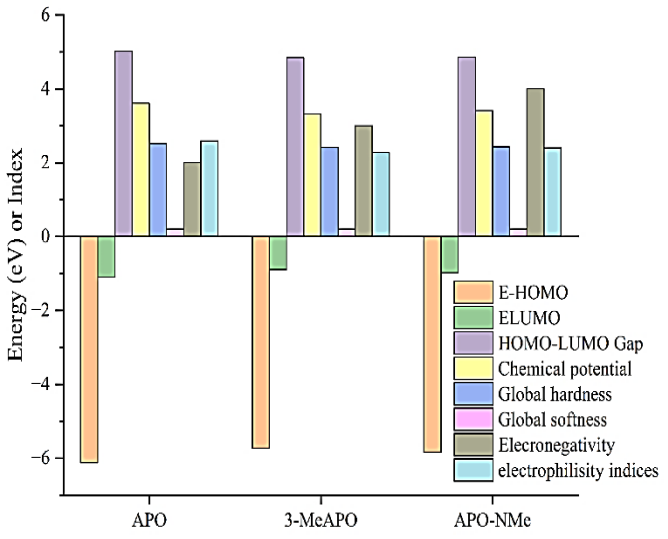

Figure 8. Electronic and global reactivity parameters for APO, APO-NMe, and 3-MeAPO.

Electrophilicity index is one of the main quantum chemical descriptors in characterizing biological or toxicity activities of the molecules in the context of the development of Quantitative Structure Activity Relationship (QSAR) parlance [٦٦-٦٤]. The computed electrophilicity indexes of APO, APO-NMe and 3-MeAPO describe the biological activity of drug-receptor interaction.

UV–visible spectral analysis

In addition, the first 10 spin-allowed singlet–singlet excitations for APO, APO-NMe and 3-MeAPO were calculated by TD-DFT approach (in gas and solution), in an attempt to understand the nature of the electronic transitions. TD-DFT calculations were started from optimized geometry using the same level of theory and performed for gas phase to calculate excitation energies. The positions of experimental and calculated absorption peaks ($\lambda_{max's}$), oscillator strengths (*f*), and major contributions of calculated transitions are given in Table 3.

In this group of compounds, the main band in the range of 300 nm can be a measure to compare the strength of the hydrogen bond. If the band tends to larger numbers (red shifts), the power of hydrogen bonding will increase. The strongest theoretical band (f=0.4649) in APO, APO-NMe and 3-MeAPO is calculated at 265 (f=0.392), 274 (f=0.448), and 276 (f=0.331) nm, respectively, which are attributed to the H→L (see Table 3). Accordingly, the IHB strength in the APO-NMe is between APO and 3-MeAPO.

Non-linear optical properties

Non-linear optical materials (NLO) have been marvelous in last years with respect to their future potential uses in the communications and photonic industries [21, 67, 68]. Urea is one of the prototypical molecules used for the study of the Nonlinear Optical (NLO) properties of molecular systems. So, it has been used frequently for comparative purposes. It is well known that the higher values of dipole moments, molecular polarizability, and hyperpolarizability are important for more active NLO properties.

Table 4
Electric dipole moment μ (Debye (D)), mean polarizability α_{tot} ($\times 10^{-24}$ esu), anisotropy polarizability $\Delta\alpha$ ($\times 10^{-24}$ esu) and first hyperpolarizability $\langle\beta\rangle$ ($\times 10^{-30}$ esu) for APO, APO-NMe and 3-MeAPO calculated at B3LYP.6-311++G(d,p) level of theory.

	APO	3-MeAPO	APO-NMe		APO	3-MeAPO	APO-NMe
μ_x	3.240	3.012	3.219	β_{xxx}	136.618	139.527	73.554
μ_y	-1.574	1.931	2.017	β_{xxy}	5.991	-29.344	2.953
μ_z	0.081	0.000	0.001	β_{xyy}	111.712	142.067	116.407
μ	3.603	3.578	3.799	β_{yyy}	55.783	-84.215	4.420
α_{xx}	-5.505	-6.510	-6.460	β_{xxz}	1.830	0.000	0.034
α_{xy}	0.863	-0.918	-0.712	β_{xyz}	3.616	0.000	-0.003
α_{yy}	-6.376	-7.620	-7.524	β_{yyz}	-2.074	0.000	0.017
α_{xz}	-0.006	0.000	0.000	β_{xzz}	-13.186	-17.513	9.861
α_{yz}	0.005	0.000	0.000	β_{yzz}	19.475	5.059	-28.174
α_{zz}	-6.726	-7.657	-7.634	β_{zzz}	5.991	0.000	0.003
α_{tot}	6.203	7.262	7.206	$\langle\beta\rangle$	2.489	2.855	2.009
$\Delta\alpha$	2.616	2.758	2.358				

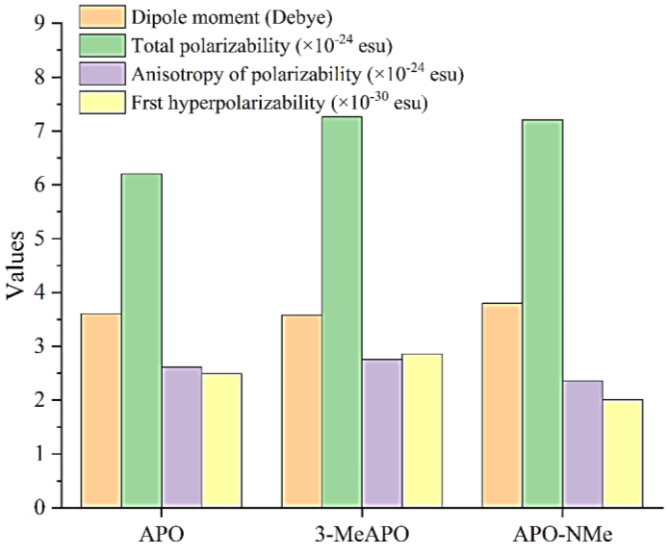

Figure 9. NLO properties comparison for APO, APO-NMe, and 3-MeAPO.

The calculated dipole moment are equal to 3.603, 3.578, 3.799 Debye (D) (see Table 4 and Figure 9.) in APO, APO-NMe and 3-MeAPO, respectively, which are biger than that to the value for urea (μ = 1.3732

D). Total polarizability (α_{tot}) and anisotropy of polarizability ($\Delta\alpha$) in APO are calculated as 6.203 and 2.616 esu. The first hyperpolarizability value β_{tot} in APO, APO-NMe and 3-MeAPO are equal to 2.489×10^{-30}, 2.855×10^{-30}, 2.009×10^{-30}esu, respectively, which are greater than that of the standard NLO material urea (μ and β of urea are 1.372 D and 0.3728×10^{-30} esu) [63]. Our title molecules with greater dipole moment and hyperpolarizability values than urea shows that the molecule has large NLO optical property.

4. Conclusion

The intramolecular hydrogen bond (IHB) strengths in 3-methyl-4-amino-3-penten-2-one (3-MeAPO) and 4-methylamino-3-penten-2-one (APO-NMe) were investigated using both theoretical and experimental approaches, including geometrical parameters, spectroscopic data, NBO, and AIM analyses. The results consistently indicate that the IHB in 3-MeAPO, with the methyl group at the α-position, is stronger than in APO-NMe, where the methyl group is attached to nitrogen. This conclusion is supported by higher N–H chemical shifts, lower N–H stretching frequencies, enhanced linearity of the O–H···O bond, and greater charge transfer interactions (LP → σ*) in 3-MeAPO. While the other results such as experimental structure and AIM results are not confirmed the above result. Overall, these findings highlight the significant role of substitution position in modulating IHB strength, which can influence the stability and reactivity of β-ketoenamine derivatives. Title compounds represented good NLO behavior.

Acknowledgments

The authors are grateful to Ferdowsi University of Mashhad and University of Mazandaran for financial support.

AuthorContributions All authors contributed equally to this work. All authors reviewed the manuscript

Declaration of Competing Interest

The authors declare that they have no known competing financial interests or personal relationships that could have appeared to influence the work reported in this paper.

Data Availability

No data was used for the research described in the article.

Funding

No funding was received to support this work.

References

[1] Jamshidvand, A., Sahihi, M., Mirkhani, V., Moghadam, M., Mohammadpoor-Baltork, I., Tangestaninejad, S., et al. Studies on DNA binding properties of new Schiff base ligands using spectroscopic, electrochemical and computational methods: Influence of substitutions on DNA-binding. J. Mol. Liq. 2018, 253, 61-71.

[2] Hansen, P.E., Kawecki, R., Krowczynski, A., Kozerski, L. Deuterium isotope effects on 13C and 15N nuclear shielding in intramolecularly hydrogen-bonded compounds. Investigation of enamine derivatives. Acta Chem. Scand. 1990, 44, 826-32.

[3] Vdovenko, S.I., Gerus, I.I., Zhuk, Y.I., Kukhar, V.P., Pagacz-Kostrzewa, M., Wierzejewska, M., et al. The conformational analysis of push-pull enaminones using FTIR and NMR spectroscopy, and quantum chemical calculations. VI. β− N− Methyl-aminovinyl trifluoromethyl ketone and α− methyl− β− N− methylaminovinyl trifluoromethyl ketone. J. Mol. Struct. 2017, 1128, 741-53.

[4] Eshghi, H., Seyedi, S.M., Safaei, E., Vakili, M., Farhadipour, A., Bayat-Mokhtari, M. Silica supported Fe (HSO4) 3 as an efficient, heterogeneous and recyclable catalyst for synthesis of β-enaminones and β-enamino esters. J. Mol. Catal. A Chem. 2012, 363, 430-6.

[5] Jeffrey, G.A., Saenger, W. Hydrogen bonding in biological structures, Springer Science & Business Media, 2012.

[6] Gilli, P., Bertolasi, V., Ferretti, V., Gilli, G. Evidence for intramolecular N− H⊙⊙⊙ O resonance-assisted hydrogen bonding in β-enaminones and related heterodienes. A combined crystal-structural, IR and NMR spectroscopic, and quantum-mechanical investigation. J. Am. Chem. Soc. 2000, 122, 10405-17.

[7] Bertolasi, V., Gilli, P., Ferretti, V., Gilli, G., Vaughan, K. Interplay between steric and electronic factors in determining the strength of intramolecular resonance-assisted NH··· O hydrogen bond in a series of β-ketoarylhydrazones. New J. Chem. 1999, 23, 1261-7.

[8] Tayyari, S.F., Raissi, H., Tayyari, F. Vibrational assignment of 4-amino-3-penten-2-one. Spectrochim. Acta A. 2002, 58, 1681-95.

[9] Hansen, P.E., Sitkowski, J., Stefaniak, L., Rozwadowski, Z., Dziembowska, T. One-bond deuterium isotope effects on 15N chemical shifts in Schiff bases. Berichtet Bunsengesel Chem. Phys. 1998, 102, 410-3.

[10] Filarowski, A., Koll, A., Rospenk, M., Krol-Starzomska, I., Hansen, P. Tautomerism of sterically hindered Schiff bases. Deuterium isotope effects on 13C chemical shifts. J. Phys. Chem. A. 2005, 109, 4464-73.

[11] Tayyari, S.F., Fazli, M., Milani-Nejad, F. Molecular conformation and intramolecular hydrogen bonding in 4-amino-3-penten-2-one. J. Mol. Struct. THEOCHEM. 2001, 541, 11-5.

[12] WEINSTEIN, J., WYMAN, G.M. A Study of β-Amino-α, β-unsaturated Ketones1. J. Org. Chem. 1958, 23, 1618-22.

[13] Buemi, G., Zuccarello, F., Venuvanalingam, P., Ramalingam, M. Ab initio study of tautomerism and hydrogen bonding of β-carbonylamine in the gas phase and in water solution. Theor. Chem. Acc. 2000, 104, 226-34.

[14] Chen, X., She, J., Shang, Z., Wu, J., Wu, H., Zhang, P. Synthesis of pyrazoles, diazepines, enaminones, and enamino esters using 12-tungstophosphoric acid as a reusable catalyst in water. Synthesis. 2008, 2008, 3478-86.

[15] Gogoi, S., Bhuyan, R., Barua, N.C. Iodine-catalyzed conversion of β-dicarbonyl compounds into β-enaminones within a minute under solvent-free conditions. Synth. Commun. 2005, 35, 2811-8.

[16] Kabak, M., Elmali, A., Elerman, Y., Durlu, T. Conformational study and structure of bis-N, N′-p-bromo-salicylideneamine-1, 2-diaminobenzene. J. Mol. Struct. 2000, 553, 187-92.

[17] Kanaani, A., Ajloo, D., Kiyani, H., Farahani, M. Synthesis, spectroscopic investigations and computational study of 4-((9, 10-dioxo-9, 10-dihydroanthracen-1-yl) oxy) benzaldehyde. J. Mol.Struct. 2014, 1063, 30-44.

[18] Moustakali-Mavridis, I.t., Hadjoudis, E., Mavridis, A. Crystal and molecular structure of some thermochromic Schiff bases. Acta Crystallogr. B. 1978, 34, 3709-15.

[19] Özek, A., Albayrak, Ç., Odabaşoğlu, M., Büyükgüngör, O. Three (E)-2-[(bromophenyl) iminomethyl]-4-methoxyphenols. Acta Cryst. Sect. C. 2007, 63, o177-o80.

[20] Yavuz, M., Tanak, H. Density functional modelling studies on N-2-Methoxyphenyl-2-oxo-5-nitro-1-benzylidenemethylamine. J. Mol. Struct. THEOCHEM. 2010, 961, 9-16.

[21] Prasad, P.N., Williams, D.J. Introduction to nonlinear optical effects in molecules and polymers, Wiley New York, 1991.

[22] Kanis, D.R., Ratner, M.A., Marks, T.J. Design and construction of molecular assemblies with large second-order optical nonlinearities. Quantum chemical aspects. Chem. Rev. 1994, 94, 195-242.

[23] Dalton, L. Nonlinear optical polymeric materials: from chromophore design to commercial applications. In: Polymers for Photonics Applications I, Springer, 2002, pp. 1-86.

[24] Fahid, F., Kanaani, A., Pourmousavi, S.A., Ajloo, D. Synthesis, tautomeric stability, spectroscopy and computational study of a potential molecular switch of (Z)-4-(phenylamino) pent-3-en-2-one. Mol. Phys. 2017, 115, 795-808.

[25] Kanaani, A., Ajloo, D., Kiyani, H., Ghasemian, H., Vakili, M., Feizabadi, M. Molecular structure, spectroscopic investigations and computational study on the potential molecular switch of (E)-1-(4-(2-hydroxybenzylideneamino) phenyl) ethanone. Mol. Phys. 2016, 114, 2081-97.

[26] Kanaani, A., Ajloo, D., Grivani, G., Ghavami, A., Vakili, M. Tautomeric stability, molecular structure, NBO, electronic and NMR analyses of salicylideneimino-ethylimino-pentan-2-one. J. Mol.Struct. 2016, 1112, 87-96.

[27] Vakili, M., Nekoei, A.-R., Tayyari, S.F., Kanaani, A., Sanati, N. Conformation, molecular structure, and intramolecular hydrogen bonding of 1, 1, 1-trifluoro-5, 5-dimethyl-2, 4-hexanedione. J. Mol.Struct. 2012, 1021, 102-11.

[28] Kanaani, A., Ajloo, D., Ghasemian, H., Kiyani, H., Vakili, M., Mosallanezhad, A. Synthesis, molecular structure, spectroscopic investigations and computational studies of (E)-1-(4-(4-(diethylamino)-2-hydroxybenzylideneamino) phenyl) ethanone. Struct. Chem. 2015, 26, 1095-113.

[29] Harris, D.C., Bertolucci, M.D. Symmetry and spectroscopy: an introduction to vibrational and electronic spectroscopy, Courier Corporation, 1989.

[30] Koşar, B., Albayrak, Ç., Ersanlı, C.C., Odabaşoğlu, M., Büyükgüngör, O. Molecular structure, spectroscopic investigations, second-order nonlinear optical properties and intramolecular proton transfer of (E)-5-(diethylamino)-2-[(4-propylphenylimino) methyl] phenol: A combined experimental and theoretical study. Spectrochim. Acta A. 2012, 93, 1-9.

[31] Seyedkatouli, S., Vakili, M., Tayyari, S.F., Hansen, P.E., Kamounah, F.S. Molecular structure and intramolecular hydrogen bond strength of 3-methyl-4-amino-3-penten-2-one and its NMe and N-Ph substitutions by experimental and theoretical methods. J. Mol. Struct. 2019, 1184, 233-45.

[32] Soltani-Ghoshkhaneh, S., Vakili, M., Berenji, A.R., Darugar, V., Tayyari, S.F. Conformations, molecular structure, and N–H··· O hydrogen bond strength in 4-Alkylamino-3-penten-2-ones. J. Mol. Struct. 2020, 1203, 127440.

[33] Bader, R. Atom in molecules a quantum theory (AIM). Encyclopedia of Computational Chemistry. 1990.

[34] Lee, C., Yang, W., Parr, R.G. Development of the Colle-Salvetti correlation-energy formula into a functional of the electron density. Phys. Rev. B 1988, 37, 785–789.

[35] Dunning Jr, T.H. Gaussian basis sets for use in correlated molecular calculations. I. The atoms boron through neon and hydrogen. J. Chem. Phys. 1989, 90, 1007-23.

[36] M.J. Frisch, G.W.T., H.B. Schlegel, G.E. Scuseria, M.A. Robb,, J.R. Cheeseman, G.S., V. Barone, B. Mennucci, G.A. Petersson,, H. Nakatsuji, M.C., X. Li, H.P. Hratchian, A.F. Izmaylov, J. Bloino,, G. Zheng, J.L.S., M. Hada, M. Ehara, K. Toyota, R. Fukuda,, J. Hasegawa, M.I., T. Nakajima, Y. Honda, O. Kitao, H. Nakai, T. Vreven,, J.A. Montgomery Jr., J.E.P., F. Ogliaro, M. Bearpark, J.J. Heyd, E. Brothers,, et al. gaussian 09, Gaussian. Inc., Wallingford CT. 2009, 150-66.

[37] Grimme, S., Antony, J., Ehrlich, S., Krieg, H. A consistent and accurate ab initio parametrization of density functional dispersion correction (DFT-D) for the 94 elements H-Pu. J. Chem. Phys. 2010, 132.

[38] Grimme, S., Ehrlich, S., Goerigk, L. Effect of the damping function in dispersion corrected density functional theory. J. Comput. Chem. 2011, 32, 1456-65.

[39] Johnson, E.R., Becke, A.D. A post-Hartree-Fock model of intermolecular interactions: Inclusion of higher-order corrections. J. Chem. Phys. 2006, 124.

[40] Karabacak, M., Cinar, M., Kurt, M. Molecular structure and vibrational assignments of hippuric acid: A detailed density functional theoretical study. Spectrochim. Acta A. 2009, 74, 1197-203.

[41] Wolinski, K., Hinton, J.F., Pulay, P. Efficient implementation of the gauge-independent atomic orbital method for NMR chemical shift calculations. J. Am. Chem. Soc. 1990, 112, 8251-60.

[42] Tomasi, J., Persico, M. Molecular interactions in solution: an overview of methods based on continuous distributions of the solvent. Chem. Rev. 1994, 94, 2027-94.

[43] Casida, M.E., Casida, K.C., Salahub, D.R. Excited-state potential energy curves from time-dependent density-functional theory: A cross section of formaldehyde's 1A1 manifold. Int. J. Quantum Chem. 1998, 70, 933-41.

[44] Reed, A.E., Curtiss, L.A., Weinhold, F. Intermolecular interactions from a natural bond orbital, donor-acceptor viewpoint. Chem. Rev. 1988, 88, 899-926.

[45] Weinhold, F., Glendening, E.D. NBO 5.0 program manual: natural bond orbital analysis programs. Theoretical Chemistry Institute and Department of Chemistry, University of Wisconsin, Madison, WI. 2001, 53706.

[46] G.A.Zhurko, D.A.Z. Chem Craft, version 1.8, http://www.chemcraf tprog.com. 2009.

[47] Darugar, V., Vakili, M., Tayyari, S.F., Hansen, P.E., Kamounah, F.S. Molecular structure, intramolecular hydrogen bond strength, vibrational assignment, and spectroscopic insight of 4-phenylamino-3-penten-2-one and its derivatives: A theoretical and experimental study. J. Mol. Liq. 2021, 334, 116035.

[48] Emamian, S., Tayyari, S.F. Theoretical study of intramolecular hydrogen bonding in the halo derivatives of 1-amino-3-imino-prop-1-ene. J. Chem. Sci. 2013, 125, 939-48.

[49] Espinosa, E., Molins, E., Lecomte, C. Hydrogen bond strengths revealed by topological analyses of experimentally observed electron densities. Chem. Phys. Lett. 1998, 285, 170-3.

[50] Snehalatha, M., Ravikumar, C. I. Hubert joe, N. Sekar, VS Jayakumar. Spectrochim. Acta A. 2009, 72, 654.

[51] Sidman, J.W. Electronic and Vibrational States of the Nitrite ION1. J. Am. Chem. Soc. 1956, 78, 2911-.

[52] Vakili, M., Darugar, V., Kamounah, F.S., Hansen, P.E., Hermann, M., Pittelkow, M. Tautomerism in pyridinyl methyl β-diketones in the liquid and the solid state; a combined computational and experimental study. J. Mol. Liq. 2023, 383, 122074.

[53] Scrocco, E., Tomasi, J. Electronic molecular structure, reactivity and intermolecular forces: an euristic interpretation by means of electrostatic molecular potentials. In: Advances in quantum chemistry, Elsevier, 1978, Vol. 11, pp. 115-93.

[54] Scrocco, E., Tomasi, J. The electrostatic molecular potential as a tool for the interpretation of molecular properties. In: New concepts II, Springer, 2005, pp. 95-170.

[55] Politzer, P., Murray, J.S. Detonation performance and sensitivity: a quest for balance. In: Adv. Quantum Chem., Elsevier, 2014, Vol. 69, pp. 1-30.

[56] Politzer, P., Murray, J. Theoretical Biochemistry and Molecular Biophysics: A Comprehensive Survey. Protein. Adenine Press, Schenectady. 1991, 2.

[57] Hush, N.S. Adiabatic rate processes at electrodes. I. Energy-charge relationships. J. Chem. Phys. 1958, 28, 962-72.

[58] Marcus, R.A. On the theory of oxidation-reduction reactions involving electron transfer. I. J. Chem. Phys. 1956, 24, 966-78.

[59] Marcus, R.A. Electron transfer reactions in chemistry. Theory and experiment. In: Protein electron transfer, Garland Science, 2020, pp. 249-72.

[60] Fukui, K. Frontier orbitals and reaction paths: selected papers of Kenichi Fukui, World Scientific, 1997.

[61] Tezer, M., Kanbul, S. Opinions of teachers about computer aided mathematics education who work at special education centers. Procedia Soc. Behav. Sci. 2009, 1, 390-4.

[62] Parr, R.G. Density functional theory of atoms and molecules. In: Horizons of Quantum Chemistry: Proceedings of the Third International Congress of Quantum Chemistry Held at Kyoto, Japan, October 29-November 3, 1979, Springer, 1989, pp. 5-15.

[63] Padmanabhan, J., Parthasarathi, R., Subramanian, V., Chattaraj, P. Electrophilicity-based charge transfer descriptor. J. Phys. Chem. A. 2007, 111, 1358-61.

[64] Chattaraj, P., Roy, D., Elango, M., Subramanian, V. Chemical reactivity descriptor based aromaticity indices applied to Al42− and Al44− systems. J. Mol. Struct. THEOCHEM. 2006, 759, 109-10.

[65] Chattaraj, P.K., Roy, D.R. Update 1 of: electrophilicity index. Chem. Rev. 2007, 107, PR46-PR74.

[66] Pérez-Garrido, A., Helguera, A.M., Guillén, A.A., Cordeiro, M.N.D., Escudero, A.G. Convenient QSAR model for predicting the complexation of structurally diverse compounds with β-cyclodextrins. Bioorg. Med. Chem. 2009, 17, 896-904.

[67] Zyss, J., Ledoux, I. Nonlinear optics in multipolar media: theory and experiments. Chem. Rev. 1994, 94, 77-105.

[68] Gilli, G., Bellucci, F., Ferretti, V., Bertolasi, V. Evidence for resonance-assisted hydrogen bonding from crystal-structure correlations on the enol form of the. beta.-diketone fragment. J. Am. Chem. Soc. 1989, 111, 1023-8.